AD_____

Award Number: W81XWH-10-1-0626

TITLE: Placental Vascular Tree as Biomarker of Autism/ASD Risk

PRINCIPAL INVESTIGATOR: Carolyn M. Salafia, M.S., M.D.

CONTRACTING ORGANIZATION: Research Foundation for Mental Hygiene
Staten Island, NY 10314

REPORT DATE: September 2012

TYPE OF REPORT: Annual

PREPARED FOR: U.S. Army Medical Research and Materiel Command
Fort Detrick, Maryland 21702-5012

DISTRIBUTION STATEMENT: Approved for Public Release;
Distribution Unlimited

# REPORT DOCUMENTATION PAGE

*Form Approved*
*OMB No. 0704-0188*



| 1. REPORT DATE | 2. REPORT TYPE | 3. DATES COVERED |
|---|---|---|
| September 2012 | Annual | 15 August 2011 – 14 August 2012 |

**4. TITLE AND SUBTITLE**

Placental Vascular Tree as Biomarker of Autism/ASD Risk

**5a. CONTRACT NUMBER**

**5b. GRANT NUMBER**
W81XWH-10-1-0626

**5c. PROGRAM ELEMENT NUMBER**

**6. AUTHOR(S)**

Carolyn M. Salafia, M.S., M.D.

Dawn P. Misra, Ph.D.; Michael Yampolsky, Ph.D.; Theresa Girardi, Ph.D.
**E-Mail:** Carolyn.Salafia@gmail.com

**5d. PROJECT NUMBER**

**5e. TASK NUMBER**

**5f. WORK UNIT NUMBER**

**7. PERFORMING ORGANIZATION NAME(S) AND ADDRESS(ES)**

Research Foundation for Mental Hygiene
Staten Island, NY 10314

**8. PERFORMING ORGANIZATION REPORT NUMBER**

**9. SPONSORING / MONITORING AGENCY NAME(S) AND ADDRESS(ES)**
U.S. Army Medical Research and Materiel Command
Fort Detrick, Maryland 21702-5012

**10. SPONSOR/MONITOR'S ACRONYM(S)**

**11. SPONSOR/MONITOR'S REPORT NUMBER(S)**

**12. DISTRIBUTION / AVAILABILITY STATEMENT**
Approved for Public Release; Distribution Unlimited

**13. SUPPLEMENTARY NOTES**

**14. ABSTRACT**

We have recently completed novel analyses of the chorionic surface vasculature in 33 Early Autism Risk Longitudinal Investigation (EARLI, high-autism risk) placentas compared 76 unselected National Children's Study (NCS) placentas. Using methods unique to our team to quantify vascular network structure, we have demonstrated, in summary, that EARLI placentas as a group show significant placental chorionic surface vascular network differences, including reduced number of chorionic surface vascular branch generations, branch and terminal vascular points and reduced mean vessel caliber as compared to NCS placentas. In addition, in EARLI placentas as a group, chorionic surface arteries, but not chorionic surface veins, terminate further from the surface perimeter, and have greater variability in that distance, and the distances between chorionic surface arteries and chorionic surface veins throughout their course on the chorionic surface are both greater and have greater variability. The placental vascular tree in ASD and in high ASD risk children, is measurably difference from controls with special education needs and controls without identified neurodevelopmental handicap.

**15. SUBJECT TERMS**
Placenta, chorionic plate, angiogenesis, autism

| 16. SECURITY CLASSIFICATION OF: | | | 17. LIMITATION OF ABSTRACT | 18. NUMBER OF PAGES | 19a. NAME OF RESPONSIBLE PERSON |
|---|---|---|---|---|---|
| a. REPORT | b. ABSTRACT | c. THIS PAGE | | | USAMRMC |
| U | U | U | UU | 31 | 19b. TELEPHONE NUMBER *(include area code)* |

**Award Number 10-1-0626**

**Table of Contents**

**ANNUAL REPORT YEAR #2**

**Award Number 10-1-0626**

**October 17, 2012**

**Program Project Title:**

CHARACTERIZATION OF THE PLACENTAL VASCULAR TREE AS A BIOMARKER OF AUTISM/ASD RISK

**Program Project PI: Carolyn M. Salafia MD, MS**

## INTRODUCTION

The overall aim of this multidisciplinary program project is to determine the correlation between patterns of placental branching growth at all levels of the placental vascular tree with diagnosis of autism/ASD as compared to diagnoses of special education needs (SEN) and "normal" outcomes, and to develop a risk assessment tool built on measures of placental shape and structure that can be performed on all infants at birth to improve identification of children who are at increased risk of autism/ASD for their early screening and diagnosis.

In this project, we are measuring and analyzing the branching of larger blood vessels on the surface of the placenta (2D), the placental shape (that contains the placental vascular fractal), and the branching structure of the fine vessels of the thickness of the placenta (3D), and correlate the maternal medical and gestational factors that may have led to differences observed between the autism/ASD group, a group of children with other special educational needs and healthy control children.

The placental examination and dissection, and the subprojects have been drawn from a nested case control study of the placental archive of the Avon Longitudinal Study of Parents and Children (ALSPAC). The proposed case group included all 56 children in the cohort with archived placentas who have been diagnosed with autism/ASD. Two control groups of children were available from the same cohort, one with SEN but not a diagnosis of autism/ASD, and one with no diagnoses related to neurodevelopmental pathology, at a 3:1 ratio to cases.

Our findings thus far include:

1. In placentas of children with ASD, there is a statistically significant difference in the chorionic surface shape, with greater maximum radius, and standard deviation of the radius of the chorionic surface shape, compared to placentas of both SEN controls and control children with neither diagnoses. This replicates our observations presented last year in the initial EARLI placentas and now confirmed in a larger sample of 87 EARLI placentas.

2. In placentas of children with ASD, there is a statistically significant greater eccentricity of the umbilical cord insertion, measured as distance of the cord insertion from the centroid of the delivered placental chorionic surface shape or defined either by the first Fourier coefficient or more directly as the distance from the cord insertion to the disk edge, as compared to placentas of both SEN controls and control children with neither diagnoses. This replicates our observations presented last year in the initial EARLI placentas and now confirmed in a larger sample of 87 EARLI placentas.

3. In placentas of children with ASD, there is a statistically significant difference in slice dimensions (note N=31 ASD cases with trace-able slice photographs compared to 79 SEN and control placentas). This is consistent with findings reported last year and now confirmed in a larger sample of 87 EARLI placentas.

4. After stratification by gender, these findings are generally preserved, although significance is attenuated among females with ASD due to the small sample size.

5. Given that there was a statistically significant reduction in placental weight (~100 g, 20% of the weight of a normal term placenta) in placentas of females with ASD cases compared to female controls, we anticipated a decrease in volume compared to both groups of controls. There was no statistically significant difference in volumes among the three groups. However, the weight to volume ratios in all groups was identical. This does not exclude does not exclude an alteration in the actual villous branching structure in female ASD (suggested by the change in beta) but resolution will require additional analysis of histologic slides.

6. The chorionic surface vasculature of placentas in 33 EARLI placentas compared to 76 National Children's Study (NCS) placentas demonstrates a reduced number of branch generations, branch and terminal vascular points, and reduced mean caliber (found in both arteries and veins). In addition, arteries, but not veins, terminate further from the surface perimeter, and have greater variability in that distance, and the distances between arteries and veins throughout their course are both greater and have greater variability.

These support our hypothesis that the placental vascular tree is altered in autism/ASD and are consistent with our findings in the EARLI cohort reported last year.

We request a no-cost extension to complete analysis of ALSPAC materials, due to the difficulties presented by the deformed condition of the placentas (see below). During 2012, time has been dedicated to development of "decrumpling" and "uncurling" methods to make these deformed placentas accessible to analysis. The no-cost extension period will be used to measure all aspects that can be reliably evaluated with existing tools in this data set, with an eye to carrying this work forward in the EARLI cohort, with well preserved placentas accessible to the measures we have validated in this grant and also with support of NIH-NCS-LOI-BIO-2-18, the National Science Foundation under Award No. DMS-1004694 and 1R43HD066952-01A1.

**BODY**

*Autism/ASD reflects a range of disordered and impaired brain development which leads to a lifelong course of behavioral and cognitive abnormalities. Diagnosis cannot formally be made prior to age two and this point there is a lack of behavioral and biologic markers that we can use to predict its onset. Early predictors could lead to early interventions which might significantly improve the lives of those affected. We intend to use the fact that the same biochemistry that controls the branching of nerves also controls branching of blood vessels. Unlike the nerve networks in the living human brain, the branching of the blood vessels in a child's placenta (that is generally discarded after birth without any examination) can be photographed and dissected. Our methods have expressly focused on capture of potentially key placental vascular features*

*using equipment and procedures that could be performed at any hospital delivering a baby in the US. Thus, if successful, our work could lead to the routine examinations of placentas at birth to provide a noninvasive newborn screening test to identify children at high risk for developing autism/ASD.*

*In this project we will measure the branching of larger blood vessels on the surface of the placenta (2D), the placental shape (that contains the placental vascular fractal), and the branching structure of the fine vessels of the thickness of the placenta (3D), and analyze the maternal medical and gestational factors that may have led to differences observed between the autism/ASD group, a group of children with other special educational needs and healthy control children. We have developed and will apply new tools to analyze digital images of placental blood vessel branching, and the mathematics required to analyze the complex patterns of this placental branching architecture. In addition to its use as a biomarker, the application of these techniques has the potential to both clarify the pathologic anatomy of autism/ASD, and to determine when during pregnancy autism/ASD might have developed.*

*Any model generated in a single population will require validation prior to its general use in public health screening. Collection of a new cohort, and confirmation of positive results from this study have been generated in each year of our award as preliminary data in families with an autistic child (in placentas of subsequently delivered infants who will begin to be able to be evaluated for autism within the next 6 months. Thus, this research is being applied in current studies of high-autism risk siblings ( EARLI., PI: Craig Newschaffer, PhD) networks, and shows early promise of being able to rapidly contribute to our understanding of likely pathways of disordered neurodevelopment in this highly heterogeneous spectrum of autism/ASD.*

***Task: Placental processing:*** *P.I.: Carolyn M Salafia, MD, NYS Institute for Basic Research in Developmental Disabilities (IBR), 1050 Forest Hill Road, Staten Island, NY, 10314. Co-Investigators: Dr Craig Charles Platt, Consultant Perinatal Pathologist and Ms Roisin Armstrong University Hospitals Bristol NHS Foundation Trust and Professor Jean Golding, Sue Ring, PhD, Mr Colin Steer, Ms Amanda Carmichael, ALSPAC, University of Bristol, Bristol, UK (no animal or human use at any of the above addresses except for use of archived anonymized placental specimens only at ALSPAC).*

*The specified placentas will be photographed and grossly processed according to protocols that Dr. Salafia previously implemented successfully in a birth cohort, and upon which placental protocols for the U.S. National Children's Study are based. These protocols will yield chorionic surface photographs that image the 2-D chorionic surface vascular tree, and serially blocked regions of the placental parenchyma from which serial sections of histologic slides can be digitized to reconstruct the 3-D (finer) chorionic vascular branched tree.*

***Timeline:*** *The 392 placentas will be fully examined, dissected and tissues processed in the first 3 months of Year 1.*

**Status:** The final placental sample size totals 348 placentas, with 53 autism/ASD cases, 145 non-ASD/non-SEN controls, and 150 SEN controls. The reasons for the change in sample size have been noted in the 2011 Annual Report.

The protocol included obtaining the following to measure placental shape and structure:

1. 3D scans of the whole placenta.

2. 2D photographs of fetal surface and the sliced placental disk.
3. Histology samples of umbilical cord, extraplacental membranes and placental villous parenchyma.

For the purposes of this proposal, the ALSPAC Executive Committee selected materials for this study not from those placentas preserved flat in casks of formalin, as was shown to the PI in multiple visits to the ASLPAC placental storage, but from a separate cohort, obtained from the private community hospital. These placentas were collected by ALSPAC staff and not preserved by the Department of Pathology. Instead they were placed in hard plastic buckets that were generally smaller in dimension than the placental chorionic plate surface. Once fixed, this resulted in generally moderate – severe deformation of this surface. The placentas were incompletely covered with formalin preservative. This, combined with ill-fitting non-air-tight bucket lids, resulted in formalin evaporation and pigment deposition on histology slides created from tissue samples of this material. This deformation of shape affected our ability to analyze 3D meshes, the 2D photographs of the placental surfaces and slices, and the formalin precipitation has rendered image segmentation of histology samples problematic.

To date, received ALSPAC placental materials include:

Total # of cases: 352

Total # with analyzable 3D scans: 179 (51%) including 63 (35%) with some degree of deformation that has been manipulated within the 3D software

Total # with deformed scans that cannot be "meshed" 114 (32%)

Total # with no 3D mesh received 59 (17%)

Total number of fetal surfaces traced 160 (45%), which is 100% of those images that can be traced, with 192 cases (55%) providing unanalyzable photographs due to surface deformation or because no photographs were received.

Total number of placental slice images traced 149 (42%)

Of note, the PI has also received and obtained 2D and 3D images and tissue samples from 137 cases from the autism/ASD family study that is the EARLI network of Drs. Craig Newschaffer and Cheryl Walker. These cases represent placentas of infants born into families with an older sibling already diagnosed with autism/ASD. While these infants have of course not been diagnosed with autism/ASD, they do reflect the placental arborization of families in which a tendency to the neuropathology that results in a diagnosis of autism/ASD has been made. As the oldest of these infants was born in late 2009, we anticipate that these children will begin to undergo tests germane to diagnoses of autism/ASD during the second year of this Innovative Idea Award and thus their placental samples can inform and extend the analyses of our principal ALSPAC cohort. Furthermore, these children have undergone extensive developmental testing at 6 and 12 months and so continuous measures of autism characteristics and precursors might also be examined prior to identification of cases. A US Department of Defense IDEA Development Award application has been submitted for this purpose.

.

***SUBPROJECT 1: ANALYSIS OF 2-D CHORIONIC SURFACE VASCULATURE***

*P.I.: Carolyn M Salafia, MD, Institute for Basic Research (IBR), 1050 Forest Hill Road, Staten Island, NY, 10314.*
*Co-Investigators: Michael Yampolsky, PhD, Department of Mathematics, University of Toronto, 105 George St, Toronto, ON M5A 2N4, Canada; Dawn P. Misra, PhD, Wayne State University, 3939 Woodward Avenue, Detroit, MI, 48201; Richard K. Miller, PhD, Department of Obstetrics and Gynecology, University of Rochester Medical Center (URMC), 601 Elmwood Avenue, Room 7-7550, Rochester, NY, 14642. (Note that there is use at any of the above addresses; use of archived anonymized digitized files only).*

*The chorionic surface vascular tree (laid down early in gestation, consistent with critical exposures periods for valproate and thalidomide on autism/ASD risk) will be extracted from the digital photographs of the chorionic surface.*

**Status**: The ***significant placental chorionic surface findings*** obtained from the EARLI cohort and reported last year has been confirmed in the ALSPAC cohort in data obtained from 2D photographs, namely that there is an increased irregularity of placental chorionic surface shape, with umbilical cord insertion sites located closer to the placental chorionic surface perimeter (more eccentric umbilical cord insertions). Our empirical models[1] and our direct research[2] indicate that both these features have their origin before the mid trimester (irregular shape) and by 11-14 weeks gestation (umbilical cord insertion).

Specifically, we have demonstrated the following:

1. In placentas of children with ASD, there is a statistically significant difference in the chorionic surface shape, with greater maximum radius, and standard deviation of the radius of the chorionic surface shape, compared to placentas of both SEN controls and control children with neither diagnoses. This replicates our observations presented last year in the initial EARLI placentas and now confirmed in a larger sample of 87 EARLI placentas.
2. In placentas of children with ASD, there is a statistically significant greater eccentricity of the umbilical cord insertion, measured as distance of the cord insertion from the centroid of the delivered placental chorionic surface shape or defined either by the first Fourier coefficient or more directly as the distance from the cord insertion to the disk edge, as compared to placentas of both SEN controls and control children with neither diagnoses. This replicates our observations presented last year in the initial EARLI placentas and now confirmed in a larger sample of 87 EARLI placentas.

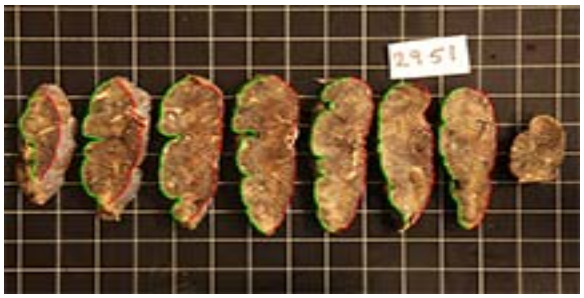


3. In placentas of children with ASD, there is a statistically significant difference in slice dimensions (note N= 31 ASD cases with trace-able slice photographs compared to 79 SEN and control placentas). This is consistent with findings reported last year and now confirmed in a larger sample of 87 EARLI placentas.
4. After stratification by gender, these findings are generally preserved, although significance is attenuated among females with ASD due to the small sample size.
5. Given that there was a statistically significant reduction in placental weight (~100 g, 20% of the weight of a normal term placenta) for female autism/ASD cases compared to female normal controls,

we anticipated a decrease in volume compared to both groups of controls. However, there was no statistically significant difference in volumes among the three groups, nor trends after stratification by gender. This does not exclude an alteration in the actual villous branching structure in female ASD (suggested by the change in beta[3,4]) but resolution will require additional analysis of histologic slides.

**Table 1. ALSPAC ASD cases compared to controls, volume derived from 3D mesh, other measures derived from 2D placental chorionic surface and slice photographs.**

| | Mean ± sd | | | |
|---|---|---|---|---|
| | Autism cases | Normal controls | Difference (autism vs. normal) | p-value |
| **Volume** | | | | |
| *Overall* | 486.7 | 518.6 | -31.9 | 0.17 |
| *Males* | 493.1 | 513 | -20.1 | 0.41 |
| *Females* | 447.2 | 552.7 | -105.5 | 0.13 |
| **Umbilical distance from centroid** | | | | |
| *Overall* | 2.97 | 3.73 | -0.75 | 0.06 |
| ***Males**** | 2.80 | 3.70 | **-0.91** | **0.04** |
| *Females* | 3.91 | 3.85 | 0.06 | 0.95 |
| **Radius minimum** | | | | |
| Overall | 5.20 | 4.58 | 0.61 | 0.13 |
| **Males*** | 5.43 | 4.52 | **0.91** | **0.04** |
| Females | 3.95 | 4.94 | -0.99 | 0.26 |
| **Radius maximum** | | | | |
| ***Overall**** | 11.98 | 13.01 | **-1.03** | **0.03** |
| ***Males*** | **11.95** | **12.96** | **-1.01** | **0.06** |
| *Females* | **12.14** | **13.30** | **-1.15** | **0.02** |
| **Radius standard deviation** | | | | |
| ***Overall**** | **2.13** | **2.65** | **-0.52** | **0.04** |
| ***Males**** | **2.02** | **2.64** | **-0.61** | **0.03** |
| *Females* | 2.70 | 2.73 | -0.04 | 0.95 |
| **Fourier 1** | | | | |
| ***Overall*** | **1.43** | **1.79** | **-0.36** | **0.052** |
| ***Males**** | **1.36** | **1.77** | **-0.42** | **0.04** |
| *Females* | 1.84 | 1.86 | -0.02 | 0.94 |
| **Fourier 2** | | | | |
| *Overall* | **0.31** | **0.39** | -0.08 | 0.08 |
| ***Males**** | **0.29** | **0.39** | **-0.10** | **0.046** |
| *Females* | 0.43 | 0.41 | 0.02 | 0.87 |
| **Perimeter** | | | | |
| *Overall* | 56.09 | 57.18 | -1.10 | 0.38 |
| *Males*<br>Unadjusted<br>Adjusted for gestational age | 56.53 | 56.98 | -0.49<br>-0.75 | 0.75<br>0.54 |
| ***Females***<br>**Unadjusted**<br>**Adjusted for gestational age** | **53.72** | **58.36** | **-4.64**<br>**-4.59** | **0.07**<br>**0.09** |
| **Area** | | | | |
| *Overall* | 233.45 | 240.82 | -7.36 | 0.44 |
| *Males* | 237.53 | 239.04 | -1.50 | 0.90 |
| ***Females*** | **211.39** | **250.69** | **-39.31** | **0.056** |

*p<0.05

**p<0.01

Negative differences == ASD cases smaller dimensions than controls.

**Table 2. 87 EARLI newborns' placentas compared to >1100 University of North Carolina Pregnancy Infection and Nutrition (UNC-PIN) Study controls, measures derived from 2D placental chorionic surface and slice photographs, EARLI data updated from 2011.**

| | UNC | EARLI | p-value |
|---|---|---|---|
| Fourier 1 | 3.23±1.81 | 3.65±2.12 | .04 |
| Displacement/Diameter | .164±.091 | .183±.112 | .06 |
| Sigma | 1.106±.492 | 2.79±1.52 | .000 |
| Symmetric Difference | 138.82±67.61 | 3519.49±2086.36 | .000 |
| Average (Avg.) Width | 2.08±.38 | 1.79±.35 | .000 |
| Linear Deviation from Avg. Width | .34±.111 | .36±.135 | .001 |
| Linear Deviation from Avg. Width Relative/Length | .020±.007 | .019±.007 | .001 |
| Average Width/Length | .125±.029 | .096±.031 | .000 |

Our study was designed to have "back-up" data sources to replicate significant findings using measures derived from a second modality, namely measures of the chorionic plate surface, cord insertion site and disk thickness and its variability extracted from 3D mesh analyses of the whole placental shape backed up by those same measures extracted from traced 2D placental chorionic surface and slice photographs. We have previously published on the association of all these measures with ultrasonographic measures at 11-14 weeks, altered birth weight, placental functional efficiency, infant gender, placental histopathology and childhood outcomes.[1, 5-15] However, our 3D mesh measures did not show statistically significant differences between placentas of ASD cases and controls, despite the numerous differences found in comparisons of 2D photographs. We are confident in our 2D findings since they have been replicated in both 3D mesh and 2D photograph measures in the EARLI cohort. In reviewing our ALSPAC measures, the analyses, and the materials from which each set of measures (2D and 3D) were derived, we have concluded that the lack of significant 3D findings is due to our methods and the assumptions inherent in the algorithms we have devised in attempts to build meshes from ALSPAC placentas that were very deformed during preservation and which rendered 3D image capture problematic.

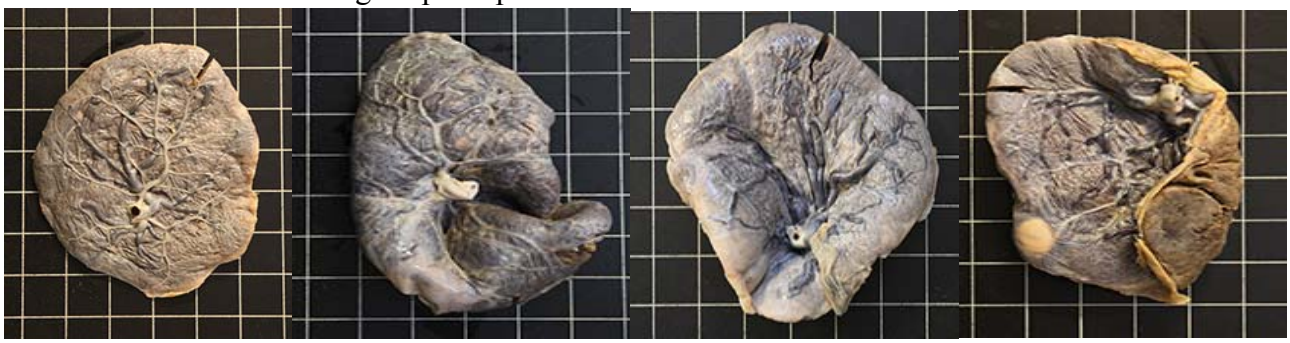

Figures (L) Flat chorionic plate surface (normal configuration), (C-R) chorionic plate surfaces of placentas deformed by preservation in poorly fit containers.

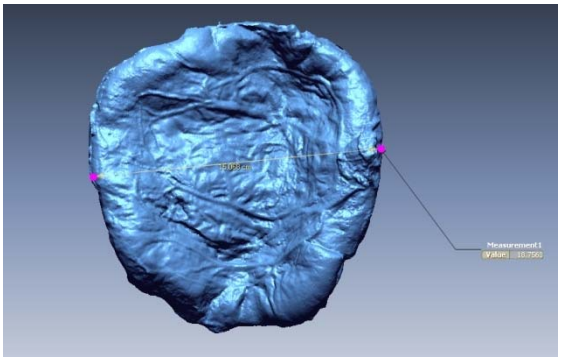

Images of the placenta mesh formed from the 3D scans: The measurement of 15.068 cm is the linear distance between the two pink points; it is the distance we would get if we only considered the 2D photo. Measurement 1 Value 19.834 is the actual distance (the geodesic distance) measured on the placenta between the two pink points. This highlights the issue of dealing with 2D photographs of placentas deformed by poorly fit containers- we cannot use the 2D photos and expect to get correct data.

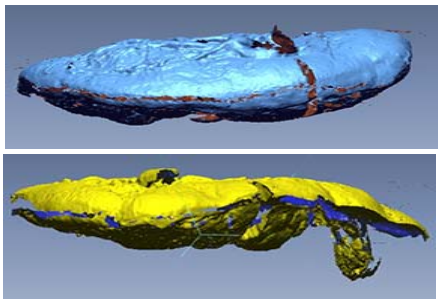

Briefly, with an undeformed placenta, after creating a 3D rendition of the placentas (a mesh), extraction of data requires gap filling in the mesh to create a closed solid from which volume and slice data can be extracted. While we have refined our mesh rendering to reduce analysis time and at the same time yield improved reconstructions from which and yielded improved reconstructions from which more and more precise shape data can be extracted, the process of gap-filling (our major time-saving step) involves certain assumptions that are more true for flat, non-deformed placentas than for the very odd configurations we have received (see Figures). One key assumption specifically depends on the chorionic plate being flat, with a more or less uniform transition from any point A to a nearby point B. For example, when the placenta is simply folded, the fetal chorionic plate may be relatively flat, while the deformation (folded edge) is far more obvious in the maternal surface images. In such a case, the top surface mesh and the bottom surface mesh cannot be merged without manual manipulation of the mesh, namely, the action of the researcher to move the fold up to a position at which it can be meshed with the top surface mesh.

Given the large number of deformed specimens, including 24 out of the 53 autism cases for which any images were received (45%), we attempted to reconstruct undeformed placental shapes in two steps, first by "uncurling" a deformed 2D placental slice, and second, by "decrumpling" a meshed placental volume.

1. ***"Slice uncurling"*** depends on the use of a parameterized curve drawn through the center of the slice. The method requires no iterations or elasticity equations. The uncurled slice measures are computed directly from the measures resulting from curve parameterization.

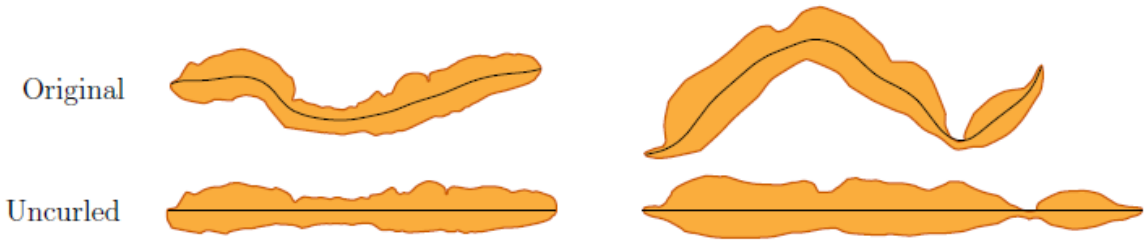


While this is an efficient approach to this question, and therefore advantageous given the hundreds of photographs to be processed, we have identified two principal problems with this approach:

Let $\gamma:[0, L] \rightarrow \mathbf{R}^2$ be an arclength parameterization of a curve which approximates the center line of a curled slice.. A method to obtain such a curve was developed previously for computing shape descriptors of a slice. Given an arbitrary point $\mathbf{Q} = [x, y]^T$ in the curled slice boundary, it can be mapped to its uncurled location $\bar{\mathbf{Q}} = [\bar{x}, \bar{y}]^T$ through the slice thickness $\delta$, local tangent $\mathbf{T}(s)$ and normal $\mathbf{N}(s)$ vectors to the curve $\gamma(s)$ using the following equation:

$$\mathbf{Q} = \gamma(s) + \mathbf{N}(s) \cdot t$$ (**Error! Reference source not found.**)

Where $s$ and $t = \frac{\delta}{2}$ are arc length parameter and normal distance from the centerline to the slice boundary at the point $\gamma(s)$; $\mathbf{T}(s) = \gamma'(s)$ is the tangent vector to the center line at the location $s$, $\|\mathbf{T}(s)\| = 1$ due to arc length parameterization; $\mathbf{N}(s) = \frac{\mathbf{T}'(s)}{\|\mathbf{T}'(s)\|}$ is the normal vector at the same location.

When slice edge is highly irregular or the thickness is close to zero, it is possible that no pair of coordinates $(s, t)$ satisfies the equation $\mathbf{Q} = \gamma(s) + \mathbf{N}(s) \cdot t$ (Error! Reference source **not found.**), or that multiple solutions exist. To avoid these situations we assume that a) center line always stays within a slice, b) slice boundaries are smoothed and don't have self-intersections and c) slice has a finite thickness.

**Algorithm**

Let $\{\mathbf{g}_n\}, n = 0, \ldots, N$ denote a sequence of points that are spaced uniformly by arc length along $\gamma$. Let $\{\mathbf{Q}_k\}$, $(k = 0, \ldots, K)$ is a sequence of points placed along curled slice boundary (e.g. upper edge).

Given $\mathbf{Q} \in \mathbf{R}^2$, we compute its uncurled location $\tilde{\mathbf{Q}} = (s, t)$ by the following algorithm.

1. We find a point $n$ on the centerline $\gamma$ where $\mathbf{Q} - \mathbf{g}_n$ is nearly perpendicular to the curve.

$$n \arg\square = \min_{n=0,\ldots,N} |(\mathbf{Q} - \mathbf{g}_n) \cdot \mathbf{g}_n'|$$

(**Error! Reference source not found.**)

Where derivatives $\gamma'$ and $\gamma''$ are estimated via finite differences as the following:

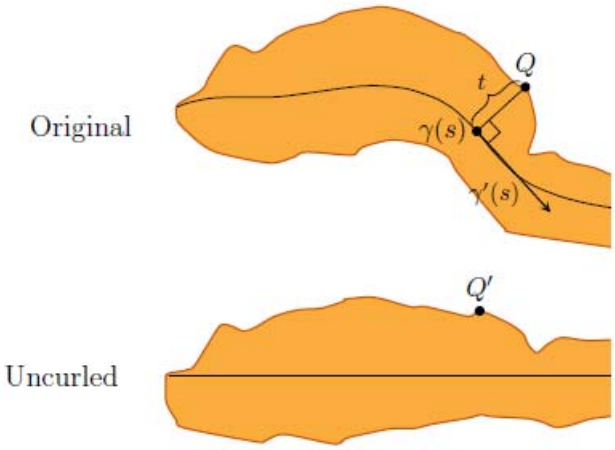


$$\mathbf{g}_n' = \frac{1}{2}(\mathbf{g}_{n+1} - \mathbf{g}_{n-1}) \qquad \mathbf{g}_n'' = \mathbf{g}_{n+1} - 2\mathbf{g}_n + \mathbf{g}_{n-1} \qquad (1)$$

2. While $n$ already provides a rough estimate of $s$, we want to further refine it in order to obtain an estimate with subsample accuracy. It can be accomplished using quadratic Taylor approximation of $\gamma$ is constructed around $n$,

$$\mathbf{P}(z) = \mathbf{g}_n + \mathbf{g}_n' z + \frac{1}{2}\mathbf{g}_n'' z^2, \qquad (-1 \le z \le 1)$$

(**Error! Reference source not found.**)

This approximation is defined such that it interpolates $\mathbf{g}_{n-1}$, $\mathbf{g}_n$, and $\mathbf{g}_{n+1}$. The value of $z$ that minimizes $\|\mathbf{Q} - \mathbf{P}(z)\|$ is selected. As it was found experimentally, that the latter gives better results than minimization of the expression $|(\mathbf{Q} - \mathbf{P}(z)) \cdot \mathbf{P}'(z)|$. Interval $z \in [-1, 1]$ corresponds to the samples $n - 1$ to $n + 1$. Therefore,

$$z \arg\square = \min_{|z| \le 1} \|\mathbf{Q} - \mathbf{P}(z)\|^2$$

(**Error! Reference source not found.**)

3. We compute values of $s$ and $t$ from $n$ and $z$, respectively.

$$s = \frac{L}{N}(n + z) \quad \text{(Error! Reference source not found.)}$$

$$t = \|\mathbf{Q} - \mathbf{P}(z)\| \quad \text{(Error! Reference source not found.)}$$

Value of $t$ is the distance between points $\mathbf{Q}$ and $\mathbf{P}(z)$ on slice boundary and the centerline curve, respectively. Corresponding point on the lower slice boundary can be found as intersection of the line $\overline{QP}$ and the lower slice boundary.

2. ***Mesh "decrumpling"*** utilizes the fact that the overall placenta shape can be well approximated by serial slices (our recent work found that even 8 slices is sufficient for volume estimation with 1.2% average error). A possible approach for decrumpling is to cut the crumpled mesh into serial slices, uncurl each slice, and then reassemble the mesh. The figure below illustrates the idea.

Crumpled Decrumpled

An implicit assumption here is that the placenta only needs to be straightened along the slice direction. This assumption is consistent with considering the placenta to behave like a developable material. That is, the placenta can bend but does not stretch or compress significantly, like a sheet of metal or cardboard.
To complete this decrumpling approach, there are points to consider:

- How to map mesh points that lie between slices (interpolation).
- How to choose the best slice direction, and can such a direction be selected automatically.

Of course, the test of any method is how well the chosen approach preserves volume, local angles, and geodesic distances.

Crumpled Decrumpled

We elected to parameterize a medial surface passing through the center of the mesh. The method is very efficient since it is computed directly, requiring no iterations or elasticity equations. However, like the "slice

uncurling" algorithm, for very irregular 3D shapes, the algorithm may yield no solution, or multiple solutions, and then the "decrumpled" volume result is arbitrary.

**Method.** Let $\gamma(u, v)$ be an approximation of the medial surface of the mesh, that is, a surface that is approximately halfway between and parallel to the fetal and maternal surfaces of the placenta. It is important that the coordinates $u$ and $v$ are unit-length parameterizations on the graph of $\gamma$. Such a surface can be efficiently constructed with polynomial surface fitting.

Given an arbitrary point Q in the original crumpled mesh, it is mapped to its decrumpled location $Q' = (u, v, w)$, where $u$, $v$, $w$ are such that

$$Q = \gamma(u, v) + \frac{\nabla\gamma(u, v)}{|\nabla\gamma(u, v)|} w.$$

Note that $\frac{\nabla\gamma(u, v)}{|\nabla\gamma(u, v)|}$ is the unit-length surface normal at $(u, v)$. As noted above, under certain circumstances, it is possible that no coordinates $(u, v, w)$ satisfy the above equation, or that multiple solutions exist.

Given a surface $z = s(x, y)$, its unit-length parameterization can be computing by

$$u(X, Y) = \int_0^X \sqrt{1 + \partial_x s(x, Y)^2}\, dx$$

$$v(X, Y) = \int_0^Y \sqrt{1 + \partial_y s(X, y)^2}\, dy$$

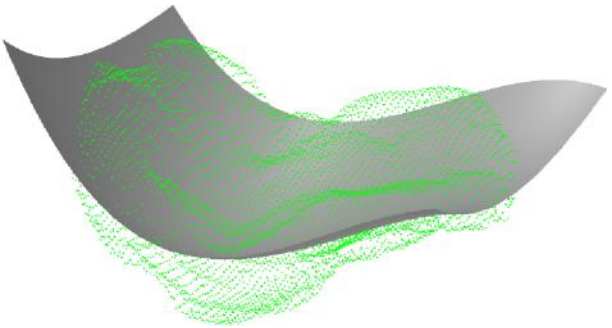

Figure 1: Green dots: points on the surface of a crumpled placenta. Gray: The medial surface 'y(u, v), created by cubic polynomial surface fitting to the points.

The following is a brief description of the algorithm:

1. Construct $\gamma$ using surface-fitting on the points of the original crumpled mesh. The example uses a cubic polynomial fit with bisquare weighting.
2. Evaluate the surface and its gradient on a grid.
3. For each point on the grid, compute the unit-length parameterizations $u(x, y)$ and $v(x, y)$.
4. For each point $Q$ in the crumpled mesh, find the closest grid point p on the surface. Adjust this value according to

$$p' = Q - \left(Q - \gamma(p)\right) \cdot \frac{\nabla\gamma(p)}{|\nabla\gamma(p)|}$$

The decrumpled location of $Q$ is $Q' = (u(p'), v(p'), w)$, where $w = (Q - p') \cdot \frac{\nabla\gamma(p)}{|\nabla\gamma(p)|}$. The values $u(p')$ and $v(p')$ are computed by cubic interpolation of the $u$ and $v$ arrays.

Finding the closest grid point *p* is time-consuming step if approached directly. A faster way to perform this search is to use a (static) spatial index. A simple spatial index that we hoped would be sufficient for our purpose is to group the grid points into square patches. The closest point is found by first finding the closest

patch and then finding the closest point within that patch (and including some overlap with adjacent patches). However, review of these assumptions will continue outside of the scope of this grant. Also, as we have noted, for both the slice uncurling algorithm (and the uncurled location $(s, t)$ and the decrumpling algorithm (for location $(u, v, w)$ under circumstances of severe deformation, which unfortunately characterizes the majority of our deformed specimens, no set of coordinates satisfies the above equation, or that multiple solutions exist. While both these algorithms may be efficient, that their solutions are ambiguous drives us to develop more precise and necessarily more demanding algorithms. This work on shape reconstruction will be continued under the aegis of 1R43HD066952-01A1 "Placental shape features, gestational timing and maternal and infant health".

During the year requested for no-cost extension, we will focus on completing the data extraction and analysis of those ALSPAC materials that are not so deformed as to require potentially ambiguous manipulations.

**Status (continued)**: S***ignificant placental chorionic surface vascular findings*** have been obtained from the chorionic surface vasculature of 33 placentas of the EARLI cohort and compared with the chorionic surface vasculature from 76 control placentas derived from the National Children's Study (NCS). EARLI placentas demonstrate a ***reduced number of branch generations***, branch and terminal vascular points reduced mean caliber (found in both arteries and veins). In addition, arteries, but not veins, terminate further from the surface perimeter, and have greater variability in that distance, and the distances between arteries and veins throughout their course are both greater and have greater variability. Branch generations on the chorionic plate surface are to a large degree determined by 11-14 weeks gestation.[7]

Our original protocol planned for the 2D chorionic surface vascular trees to be transformed in a series of 2D coordinates that represent points sampled along arbors (or paths) of chorionic vessels with the branching information. This skeletonization had been accomplished, with the processing of those networks into a series of 2D coordinates that represent points sampled along arbors (or paths) of chorionic vessels with the branching information. The graph of the placental chorionic vasculature includes the graph nodes from the labeled branch

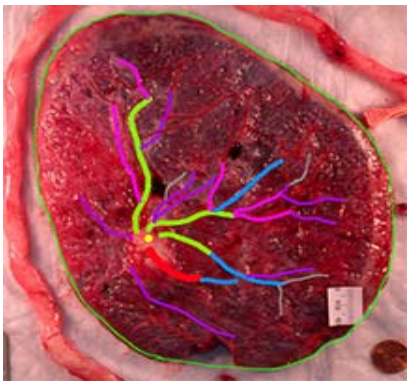

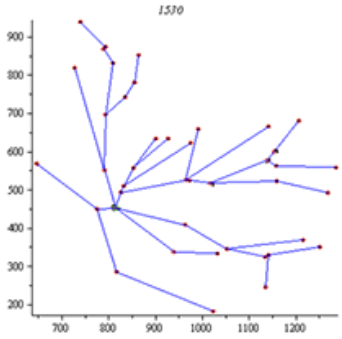


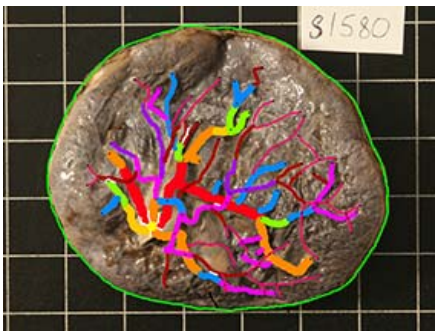


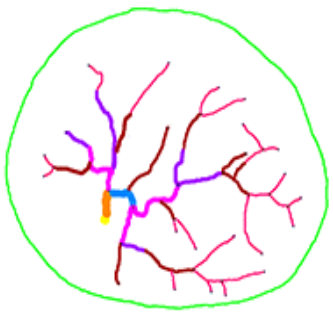

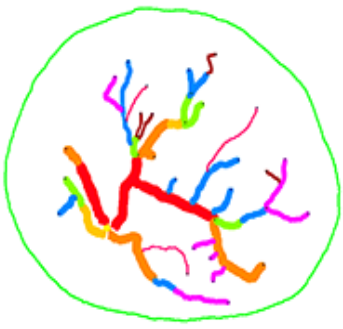

points and the graph edges based from the connecting vessel tracing lines, which also codes vascular diameters. In the line drawing, it is clear that the true vascular lengths, including interbranching intervals

(marking cell division rates intervening between genetic triggering of vascular branching), are underestimated.

Our current algorithm for vascular skeletonization is a significant improvement over our previous method since vessel curvature and accurate vessel lengths, as well as true distances between vessel segments, can be analyzed.

As noted above, the chorionic vascular distributions of arteries and veins, generations of branching, distribution on the chorionic surface, relative to the perimeter and to each other, were each significantly different in EARLI, indicating sparser vasculature with decreased branching, extension and surface distribution relative to the NCS placentas, obtained from a population of unselected healthy deliveries at term. Below left is an "average" NCS placental surface vascular network extracted using our protocol, center an EARLI placental surface vascular network 1SD above the mean density, and right, an "average" EARLI placental surface vascular network.

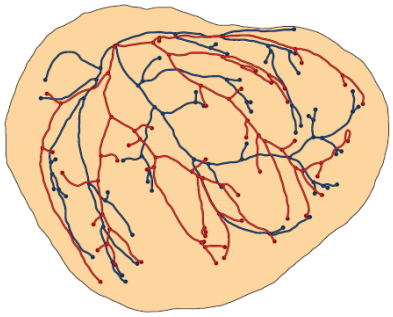
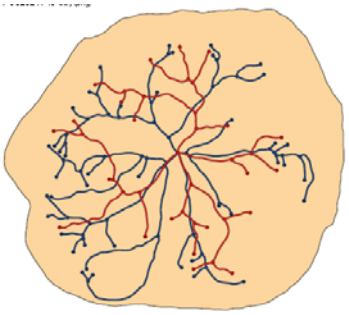
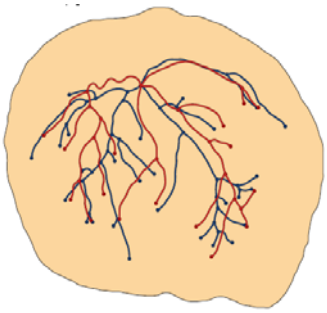

**Table 3. Vascular measures of chorionic surface networks, comparison of EARLI and NCS placentas.**

| NCS N= 76<br>EARLI N= 33 | Arteries | | | | | Veins | | | | |
|---|---|---|---|---|---|---|---|---|---|---|
| | Mean | SD | Min | Max | Sig. | Mean | SD | Min | Max | Sig. |
| Number of generations | | | | | .000 | | | | | .019 |
| NCS | 8.89 | 1.69 | 5 | 13 | | 9.24 | 2.14 | 1 | 5 | |
| EARLI | 7.36 | 1.73 | 3 | 11 | | 8.18 | 1.85 | 5 | 13 | |
| Number of branch points | | | | | .000 | | | | | .065 |
| NCS | 30.16 | 11.03 | 8 | 68 | | 32.91 | 11.96 | 10 | 86 | |
| EARLI | 20.42 | 8.12 | 4 | 38 | | 27.88 | 9.14 | 10 | 48 | |
| Number of end points | | | | | .000 | | | | | .05 |
| NCS | 32.80 | 11.12 | 11 | 71 | | 35.99 | 11.97 | 12 | 88 | |
| EARLI | 23.03 | 8.26 | 6 | 41 | | 30.94 | 9.12 | 13 | 53 | |
| Arc length | | | | | .003 | | | | | .21 |
| NCS | 109.40 | 27.68 | 39 | 186 | | 117.58 | 28.26 | 41 | 182 | |
| EARLI | 91.05 | 23.18 | 38 | 130 | | 108.86 | 27.64 | 57 | 163 | |
| Mean vessel width | | | | | .000 | | | | | .000 |
| NCS | .15 | .03 | .08 | .25 | | .19 | .06 | .08 | .42 | |
| EARLI | .19 | .04 | .14 | .31 | | .25 | .05 | .16 | .38 | |
| Variability in vessel width | | | | | .000 | | | | | .000 |
| NCS | .09 | .02 | .04 | .17 | | .11 | .03 | .04 | .20 | |
| EARLI | .11 | .03 | .07 | .23 | | .15 | .04 | .09 | .24 | |
| Mean distance from vessel to perimeter | | | | | .008 | | | | | .176 |
| NCS | 2.25 | .48 | 1.33 | 4.50 | | 2.16 | .48 | 1.36 | 4.3 | |
| EARLI | 2.51 | .72 | .00 | 4.12 | | 2.21 | .60 | .00 | 3.4 | |
| Variability in mean distance from vessel to perimeter | | | | | .01 | | | | | .46 |
| NCS | .75 | .22 | .43 | 1.49 | | .76 | .20 | .42 | 1.3 | |
| EARLI | .85 | .28 | .00 | 1.45 | | .80 | .34 | .00 | 1.9 | |
| Mean distance from vessel end | | | | | .007 | | | | | .34 |

| | | | | | | | | | | |
|---|---|---|---|---|---|---|---|---|---|---|
| point to perimeter | | | | | | | | | | |
| NCS | 2.43 | .50 | 1.57 | 4.77 | | 2.35 | .51 | 1.53 | 4.9 | |
| EARLI | 2.76 | .83 | .00 | 4.21 | | 2.43 | .71 | .00 | 3.8 | |
| Variability in mean distance from vessel end point to perimeter | | | | | .001 | | | | | .44 |
| NCS | .79 | .21 | .46 | 1.48 | | .81 | .22 | .44 | 1.47 | |
| EARLI | .98 | .36 | .00 | 1.70 | | .85 | .33 | .00 | 1.8 | |

| | Mean | St. Dev. | Min | Max | Sig. |
|---|---|---|---|---|---|
| Mean distance from an artery end point to a venous endpoint | | | | | .000 |
| NCS | .86 | .18 | .56 | 1.37 | |
| EARLI | 1.17 | .35 | .72 | 2.00 | |
| Variability in distance from an artery end point to a venous endpoint | | | | | .009 |
| NCS | .73 | .16 | .43 | 1.12 | |
| EARLI | .89 | .28 | .52 | 1.50 | |
| ALSPAC | | | | | |
| Mean distance from any artery to the nearest vein | | | | | .040 |
| NCS | .50 | .08 | .33 | .70 | |
| EARLI | .59 | .19 | .37 | 1.09 | |
| ALSPAC | | | | | |
| Variability in distance from any artery to the nearest vein | | | | | .004 |
| NCS | .38 | .08 | .23 | .64 | |
| EARLI | .49 | .20 | .27 | 1.07 | |
| ALSPAC | | | | | |

The often deformed chorionic plate surfaces have made such analyses in ALSPAC more fraught; the moderately deformed placental chorionic surface had two photographs provided, one as shown and one with four hands holding down the perimeter of the disk. This manipulation resulted in a 33% increase in the measured chorionic surface area, but only a 15-20% increased in measured venous and arterial total length, respectively. However, the number of branch generations and branch points in this specimen were unchanged, as was the mean measured vessel width and the mean distance from vessel end points to the chorionic surface perimeter. As was the case last year, EARLI leads the way for focused measurement and optimal utilization of the problematic ALSPAC materials. In addition, a number of features that distinguish EARLI from NCS placentas, such as the surface vascular density, and the distance from vessel termination to the disk perimeter are accessible to automated extraction from 2D photographs (L), especially when polarizing filters remove glare (C), or from 3D meshes (of undeformed placentas, R).

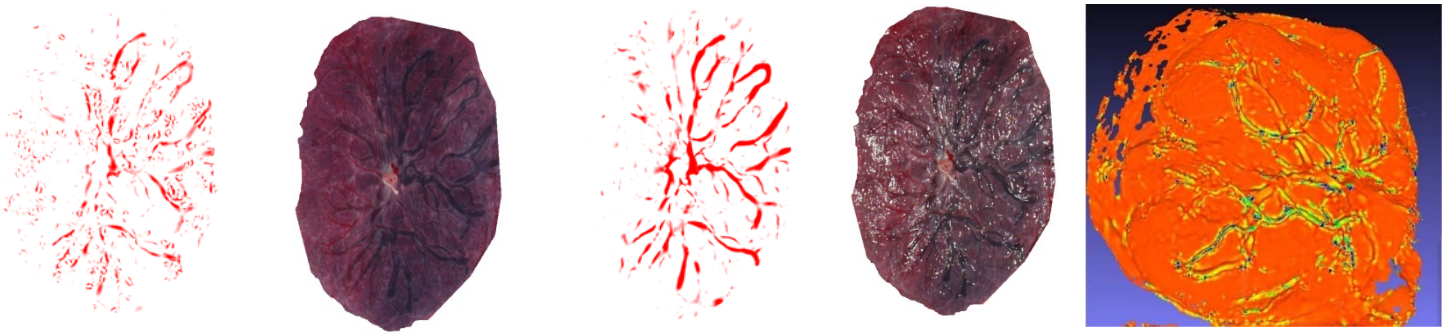

**Timeline:** We will complete data extraction from the last usable images by 12/2012.

**Accomplishments for this Subproject**

1. Significant differences in placental chorionic surface shape (reflecting lateral chorionic vascular extension), and placental disk thickness initially identified in the first EARLI family placentas analyzed in

2011 have been confirmed in the ALSPAC cohort. This supports the hypothesis that deviations in placental angiogenesis are correlated with ASD as diagnosed in ALSPAC and can be also demonstrated in placentas of EARLI newborns who have not yet been diagnosed with ASD. Future exciting research will determine whether the differences in EARLI placentas are confined to that percentage of children in such high risk families who will eventually be diagnosed with ASD by 2 years of age, or whether high-risk families have global and basic differences in angiogenesis (in which case EARLI newborns will share deviations from the standard patterns of vascular growth we have documented in low-risk birth cohorts). This will allow more targeted investigation of genes and gene-environment interactions in gestation that may be central to genesis of ASD risk.

2. Additional cases from the EARLI project continue to be incorporated into this project at no additional cost.

## *SUBPROJECT 2: 3D RECONSTRUCTION OF PLACENTAL VOLUME AS A PROXY FOR THE SHAPE OF THE CHORIONIC VASCULAR TREE*

***3D reconstructions of placental volume as a proxy for the shape of the chorionic vascular tree***
*Placental shapes, as captured in surface and slice images in the form of 3-D coordinate data, are created by rotating and translating the hand-traced 2D contours coordinates. Geometric descriptors will be easily extracted from the reconstructed shapes, such as surface area, volume, mean curvature, total curvature, shape moments, deviation from an average-shaped placenta, etc. These values will then be used in a classification approach, finding signatures for normal or abnormally shaped placentas, and to link these with our outcomes.*

*Chang [8] showed that 2D shape information of the placenta is meaningful for health prediction: "initial findings indicate significant relationships between shape of the placental surface and newborn's birth weight as well as their gestational age." Therefore, since 3D shape information is a superset of what is available in 2D, one would expect that health prediction based on 3D shape information would be even better, and is certainly merits investigation.*

***3D reconstructions of finer placental branching vasculature*** *Sets of blocks obtained from placental parenchyma centered on a diving chorionic placental vessel will be serially sectioned as follows: Slides 1-3 H&E, 4-5 retained for possible future immunohistochemistry (IHC) stains, 6-8 stained with H&E, 9-10 retained unstained, etc.*

1. *The stained slides will be digitized and the series registered using standard registration techniques. Since villous branching is driven by vascular branching in the fetal systems, we need only to register the (larger) villus, simplifying the task of registration.*
2. *The registered 3D structure will be pruned of the terminal villi, development of which is by simple capillary extension and therefore do not reflect the mechanism of growth we are targeting. This radically simplifies the fine chorionic vascular tree.*
3. *These 3D networks will be transformed and analyzed as in Subproject 1, above.*

**Status**: We reported in last year's Annual Report that there was a statistically significant reduction in placental weight (~100 g, 20% of the weight of a normal term placenta) in placentas of females with ASD cases compared to female controls. We therefore anticipated a decrease in volume in females with ASD compared to both groups of female controls and to all male groups. There was no statistically significant difference in volumes among the groups. Consistent with this, the weight to volume ratios in all groups was identical (data not shown). This does not exclude an alteration in the actual villous branching structure in female ASD (suggested by the change in beta) but resolution of the finding of a significantly different beta, and reduced placental weight without a change in volume density will require analysis of histologic slides.

As a proxy for the arborization of villous fetal stem branches, we have identified significant differences in disk thickness and thickness variability in ASD as compared to controls in the ALSPAC cohort, and in EARLI placentas compared to those of a low-risk birth cohort. However, our attempts to view the villous tree at the microscopic level in its full complexity have proved problematic. Our proposal goals were to perform color image segmentation and register serial sections in order to reproduce a virtual placental fetal

stem villous "tree" that could be directly measured as a network. The color image segmentation of routinely stained hematoxylin and eosin stained slides was expected to be difficult:

- aging of tissues after 20 years preservation in formalin alters staining characteristics of key components, especially loss of the normal red-orange staining of erythrocytes and instead a pale pink coloration of these cells that is virtually indistinguishable from connective tissue
- formalin evaporation precipitates opaque black formalin on tissues, obscuring tissue details and further complicating segmentation.

However, we planned to develop these techniques in contemporaneous specimens (with good technical preservation) with the hope that they could then be modified for the specific challenges of ALSPAC tissues.

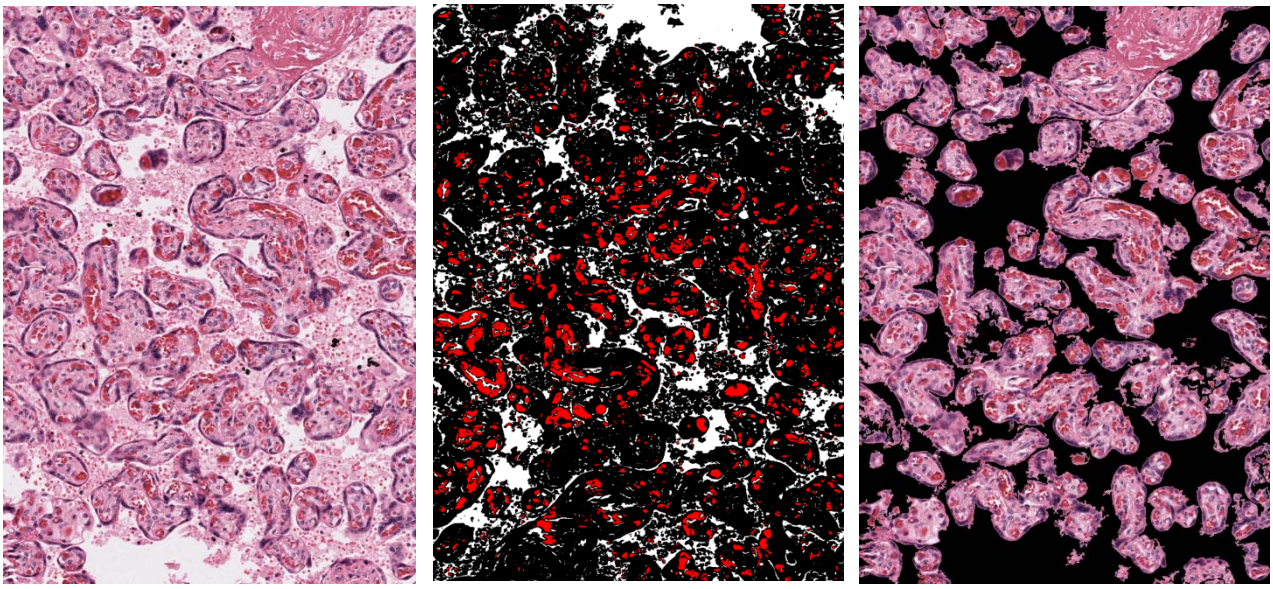

The basic principle that we use for segmentation is that the slide background is white. Thus, an approach is to determine for every pixel a scalar quantity describing how white that pixel is, and then comparing this quantity to a threshold. The details then are in how to compute the scalar quantity and how to set the threshold. For different applications and purposes, we adapt suitable thresholds and quantity for the specific characteristics.

Approximately 10 serial sections were registered to create a "movie". However, the Institute of Pure and Applied Mathematics (IPAM) and the University of California, Los Angeles, was unable to register more sections, or to "prune" them of the distal terminal villi to reveal the dichotomous branching fetal stem structure. Additionally, when we attempted to replicate the segmentation above (R) provided to us by IPAM, it became apparent that significant post-processing (manual correction) had been involved in the generation of that image.

The PI continues to pursue the work with Definiens initially presented in 2008, but edge detection of complex villous trees remains problematic in routine stained slides. Maternal blood cells often fill the intervillous space, obliterating the white "space" upon which we would base detection of the villous edge. We will continue to pursue this path toward placental villous image segmentation outside of the scope of this year of no-cost extension.

However, in order to complete our tasks, we have elected to use different villous images to render segmentation a far simpler task, by use of cytokeratin immunohistochemistry staining. The four images below show routine staining and cytokeratin immunohistochemistry at 4x and 20x magnifications. At even 20x magnification, the villi are crowded and intervillous (maternal) erythrocytes make distinction of villous

boundaries (essential for villous segmentation) problematic. However, cytokeratin immunohistochemistry outlines the villous borders, does not stain maternal or fetal erythrocytes, and thus drastically simplifies segmentation.

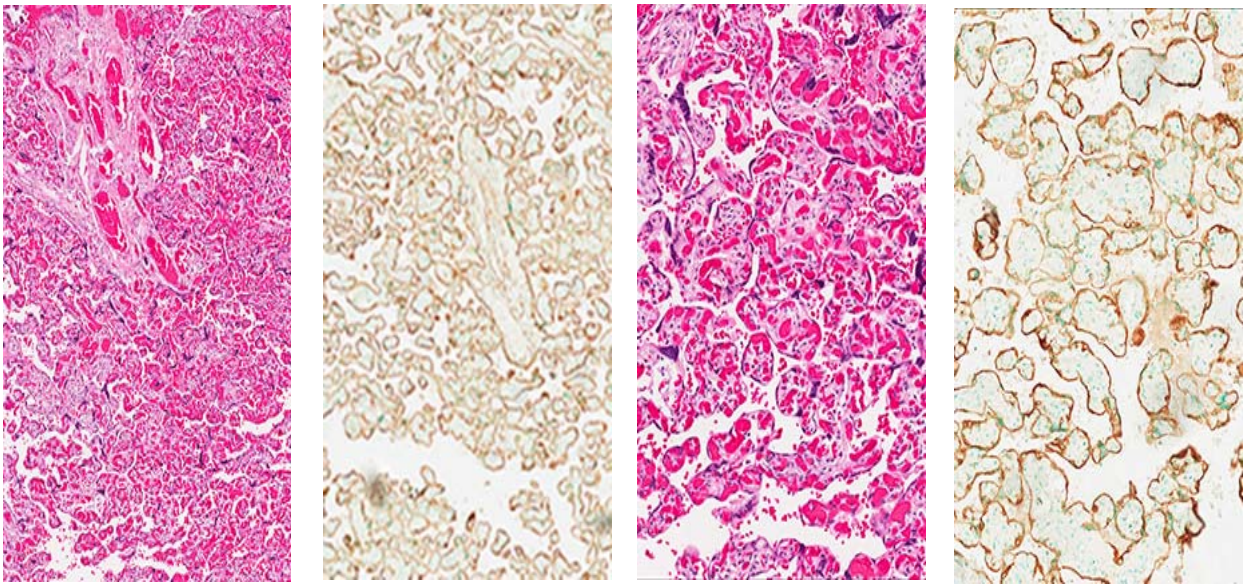

We have developed a specific algorithm for the segmentation of the digital immunohistochemistry stains, which segments the brown staining identifying cytokeratin, After the brown staining is segmented, random fluctuations are removed to streamline the shapes. This will facilitate consistent and objective analysis of size and shape.

***SUBPROJECT 3: EPIDEMIOLOGY OF GESTATIONAL MODIFIERS OF PLACENTAL VASCULAR STRUCTURE AND ASD RISK***

*P.I: W. Ted Brown, MD, PhD, IBR; Co-Investigators: Carolyn M Salafia, MD, IBR; Eric London, MD, IBR; Dawn P. Misra, PhD, Department of Family Medicine and Public Health Services, Wayne State University School of Medicine, 101 E. Alexandrine, Room #203, Detroit, MI, 48201 (no animal or human use at any of the above addresses; use of archived anonymized data only).*

This will be completed within the time period of the no-cost extension.

**KEY RESEACH ACCOMPLISHMENTS**

This project has been proceeding well. We have, at no additional cost, continued to incorporate EARLI high-risk newborn's placentas into data analysis, which in Year 1 provided our first evidence supporting the hypothesis that placental structure is measurably different in ASD cases, as well as potentially in their families, reflecting genetic predisposition to altered patterns of angiogenesis or altered susceptibility to factors that modify angiogenesis. Methods for volume reconstruction and estimation from 3D mesh and 2D photographs have been validated in the National Children's Study, a significant cost savings to this project.

1. In placentas of children with ASD, there is a statistically significant difference in the chorionic surface shape, with greater maximum radius, and standard deviation of the radius of the chorionic surface shape, compared to placentas of both SEN controls and control children with neither diagnoses. This replicates our observations presented last year in the initial EARLI placentas and now confirmed in a larger sample of 87 EARLI placentas.

2. In placentas of children with ASD, there is a statistically significant greater eccentricity of the umbilical cord insertion, measured as distance of the cord insertion from the centroid of the delivered placental chorionic surface shape or defined either by the first Fourier coefficient or more directly as the distance from the cord insertion to the disk edge, as compared to placentas of both SEN controls and control children with neither diagnoses. This replicates our observations presented last year in the initial EARLI placentas and now confirmed in a larger sample of 87 EARLI placentas.

3. In placentas of children with ASD, there is a statistically significant difference in slice dimensions (note N=31 ASD cases with trace-able slice photographs compared to 79 SEN and control placentas). This is consistent with findings reported last year and now confirmed in a larger sample of 87 EARLI placentas.

4. After stratification by gender, these findings are generally preserved, although significance is attenuated among females with ASD due to the small sample size.

5. Given that there was a statistically significant reduction in placental weight (~100 g, 20% of the weight of a normal term placenta) in placentas of females with ASD cases compared to female controls, we anticipated a decrease in volume compared to both groups of controls. However, there was no statistically significant difference in volumes among the three groups. This suggests that the placentas of girls with autism, which weigh less, but occupy the same volume, are "built" differently, with relatively reduced branches despite similar length of long fetal stem anchoring villi. This would be consistent with our previous finding of an alteration in beta, a measure of the integrity of the placental vascular fractal in autism/ASD cases compared to female normal controls.

6. The chorionic surface vasculature of placentas in 33 EARLI placentas compared 76 National Children's Study (NCS) placentas demonstrates a reduced number of branch generations, branch and terminal vascular points reduced mean caliber (found in both arteries and veins). In addition, arteries, but not veins, terminate further from the surface perimeter, and have greater variability in that distance, and the distances between arteries and veins throughout their course are both greater and have greater variability.

**REPORTABLE OUTCOMES**

1. In placentas of children with ASD, there is a statistically significant difference in the chorionic surface shape, with greater maximum radius, and standard deviation of the radius of the chorionic surface shape, compared to placentas of both SEN controls and control children with neither diagnoses. This replicates our observations presented last year in the initial EARLI placentas and now confirmed in a larger sample of 87 EARLI placentas.

2. In placentas of children with ASD, there is a statistically significant greater eccentricity of the umbilical cord insertion, measured as distance of the cord insertion from the centroid of the delivered placental chorionic surface shape or defined either by the first Fourier coefficient or more directly as the distance from the cord insertion to the disk edge, as compared to placentas of both SEN controls and control children with neither diagnoses. This replicates our observations presented last year in the initial EARLI placentas and now confirmed in a larger sample of 87 EARLI placentas.

3. In placentas of children with ASD, there is a statistically significant difference in slice dimensions (note N=31 ASD cases with trace-able slice photographs compared to 79 SEN and control placentas). This is consistent with findings reported last year and now confirmed in a larger sample of 87 EARLI placentas.

4. After stratification by gender, these findings are generally preserved, although significance is attenuated among females with ASD due to the small sample size.

5. Given that there was a statistically significant reduction in placental weight (~100 g, 20% of the weight of a normal term placenta) in placentas of females with ASD cases compared to female controls, we anticipated a decrease in volume compared to both groups of controls. There was no statistically significant difference in volumes among the three groups. However, the weight to volume ratios in all groups was identical. This does not exclude does not exclude an alteration in the actual villous branching structure in female ASD (suggested by the change in beta) but resolution will require additional analysis of histologic slides.

6. The chorionic surface vasculature of placentas in 33 EARLI placentas compared 76 National Children's Study (NCS) placentas demonstrates a reduced number of branch generations, branch and terminal vascular points reduced mean caliber (found in both arteries and veins). In addition, arteries, but not veins, terminate further from the surface perimeter, and have greater variability in that distance, and the distances between arteries and veins throughout their course are both greater and have greater variability.

**Presentations:**
**Abstracts of ALSPAC and EARLI chorionic disk and slice results were presented at the International Federation of Placenta Association Meeting, Hiroshima, Japan, September 2012, and the EARLI chorionic vascular data has been submitted for presentation at the Society for Gynecological Investigation (SGI) meeting in March 2013.**

***Presented at the International Federation of Placental Associations meeting, published in Placenta (Suppl) 2012.***

**Characterization of Placental Growth as a Biomarker of Autism/ASD Risk** C Salafia[1,2], D Misra[3], J Golding[4], C Platt[5], S Ring[4]
1Institute for Basic Research, Staten Island, NY, United States, 2Placental Analytics, LLC, Larchmont, NY, United States, 3Wayne State University School of Medicine, Detroit, MI, United States, 4University of Bristol, Bristol, UK, and 5University Hospital's Bristol NHS Foundation Trust, Bristol, UK.

**Aims and Background:**The Avon Longitudinal Study of Parents and Children (ALSPAC) is a long-term health research project. More than 14,000 mothers enrolled during pregnancy in 1991 and 1992, and the health and development of their children has been followed in great detail ever since. The ALSPAC families have provided a vast amount of genetic and environmental information over the years. This resource is assisting scientists all over the world with research into a wide range of health problems. The aim of this particular research was to determine the correlation between placental growth patterns with diagnosis of autism/ASD as compared to a control group.
**Methods:** A nested case control study of the Avon Longitudinal Study of Parents and Children (ALSPAC) included archived placentas for 52 children (7 female, 45 male) in the cohort with diagnosed with autism/ASD and for a control group (N=161) with no neurodevelopmental diagnoses, at a 3:1 ratio to cases.
**Results:** 1. Placental weight was significantly reduced (~100 g) in female autism cases compared to controls, also after adjusting for gestational age ($p<0.05$). This was not the result of outliers in either distribution. No such effects were seen in males.
2. The influence of gestational age on placental weight differed by sex in regression models to predict placental weight by case/control status and gestational age. Gestational age had a strong effect on placental weight for males ($p<0.05$) but not for females; we did not test the interaction due to the small sample.
3. The smaller placental dimension did not significantly differ between autism cases and controls in either gender. However, the difference among females (-1.41 cm) was two-fold that of males (-018 cm).
4. A marker of placental functional efficiency and placental fractal structure, did not differ between boys with autism/ASD (0.755+0.0239) and controls (0.753+0.0202). Beta differed between girls with and without autism/ASD (0.733+0.0354 v. 0.760+0.0161, p=0.001). b differed by gestational age only in boys (point estimate of effect=-0.002, p=0.009 v. females with p=0.53). The association of altered b in girls with autism/ASD persisted after adjustment for gestational age (estimate of effect of autism/ASD "case" status=0.03, p=0.01).

| | Mean ± sd | | | |
|---|---|---|---|---|
| | ASD cases | Controls | Difference (ASD vs. control) | p-value |
| ***Placental weight (g)*** | | | | |
| ***Overall*** | 469.2 ± 112.4 | 478.1 ± 100.4 | -8.87 | 0.59 |
| *Males*<br>Unadjusted<br>Adjusted for GA Term (≥37 weeks gestation) | 480.52 ± 103.9 | 475.52 ± 101.20 | +4.99<br>+3.86<br>+0.92 | 0.77<br>0.81<br>0.96 |
| *Females*<br>Unadjusted*<br>Adjusted for GA* Term (≥37 weeks gestation)* | 395.00 ± 145.23 | 495.10 ± 95.40 | -100.10<br>-99.62<br>-100.10 | 0.045<br>0.050<br>0.045 |
| ***Larger placental dimension (cm)*** | | | | |
| *Overall* | 18.20 ± 3.19 | 18.75 ± 2.15 | -0.55 | 0.26 |
| *Males* | 18.28 ± 3.00 | 18.80 ± 2.26 | -0.52 | 0.29 |
| *Females* | 17.71 ± 4.51 | 18.45 ±1.35 | -0.74 | 0.59 |
| ***Smaller placental dimension (cm)*** | | | | |
| *Overall* | 16.51 ± 2.48 | 16.85 ± 1.93 | -0.34 | 0.32 |
| *Males* | 16.74 ± 2.50 | 16.92 ±1.97 | -0.18 | 0.63 |
| *Females* | 15.04 ± 1.88 | 16.45 ± 1.70 | -1.41 | 0.08 |
| ***Placental functional efficiency (β)*** | | | | |
| *Overall* | 0.7516 ± 0.026 | 0.7539 ± 0.019 | -0.0023 | 0.56 |
| *Males*<br>Unadjusted<br>Adjusted for GA | 0.7545 ± 0.024 | 0.7530 ± 0.023 | +0.0016<br>+0.002 | 0.67<br>0.62 |
| *Females*<br>Unadjusted**<br>Adjusted for GA** | 0.7333 ± 0.035 | 0.7604 ± 0.016 | -0.0270<br>-0.0270 | 0.009<br>0.010 |

**Conclusions**: Gestational age effects on autism/ASD risk may be marked by altered placental fractality and vascular structure. We hypothesize that placental growth patterns are altered in autism/ASD in gender specific fashions which may provide insights into the mechanisms of and differences between autism/ASD frequency and phenotype in females compared to males.

**Analysis of placental shape and cord insertion in a related cohort of familial autism, the EARLI cohort.**

M Yampolsky[1], O Shlakhter[1], D Misra[2], C Salafia[3,4]
[1]University of Toronto, Toronto, Canada, [2]Wayne State University School of Medicine, Detroit, MI, United States, [3]Institute for Basic Research, Staten Island, NY, United States, [4]Placental Analytics, LLC, Larchmont, NY, United States.

**Aims:** To determine the correlation between placental growth patterns of high risk sibling from families with an older child diagnosed with autism/ASD as compared to a large and well-studied birth cohort.
**Methods:** 53 well preserved digital photographs of the fetal surface and 51 digital photographs of the sliced placental disk from EARLI high autism risk newborns been processed identically to the University of North Carolina Pregnancy, Infection and Nutrition Study (UNC PIN), extensively analysed by the PI and are treated here as the reference group for the EARLI placentas. Fourier analysis of the shape and cord displacement (calculated as the displacement from the center of the area of the chorionic plate shape) of the two groups were compared using non-parametric correlations with $p<0.05$ significant.
**Results:** Umbilical cord marginality defined either by the first Fourier coefficient or more directly as the cord displacement differs significantly between autism/ASD cases and the UNC PIN birth cohort. Cord displacement is greater in placentas from siblings of autism/ASD cases; cords are closer to the placental chorionic disk margin. The disks of autism/ASD case siblings are less round, more irregular in perimeter, with significantly larger values of sigma and symmetric difference and measures of placental roundness (each $p<0.0001$). Disk thickness in autism/ASD siblings was also significantly less ($p<0.0001$) as was the linear deviation from the average width (a measure of thickness variability, [2]). This finding was independent on the length of the slice (diameter of placental disk).
**Conclusion:** These data show early promise of being able to use placental measures to contribute to our understanding of likely pathways of disordered neurodevelopment in the heterogeneous spectrum of autism/ASD.

| | Mean ± standard dev. | | | |
|---|---|---|---|---|
| | UNC | EARLI | Difference (UNC vs. EARLI) | p-value |
| Fourier 1 | 3.231±1.817 | 4.069±2.345 | -.838 | .015 |
| Displacement | 3.455±1.911 | 4.228±2.515 | -.773 | .040 |
| Displacement/Diameter | .164±.091 | .204±.122 | -.040 | .029 |
| Sigma | 1.106±.492 | 3.104±1.696 | -1.998 | .000 |
| Symmetric Difference | 138.815±67.609 | 3519.491±12086.36 | -220.676 | .000 |
| Average (Avg.) Width | 2.076±.382 | 1.853±.366 | .223 | .000 |
| Linear Deviation from Avg. Width | .340±.111 | .368±.148 | -.028 | .000 |
| Linear Deviation from Avg. Width Relative/Length | .020±.007 | .019±.008 | .001 | .005 |
| Average Width/Length | .125±.029 | .100±.035 | .025 | .110 |

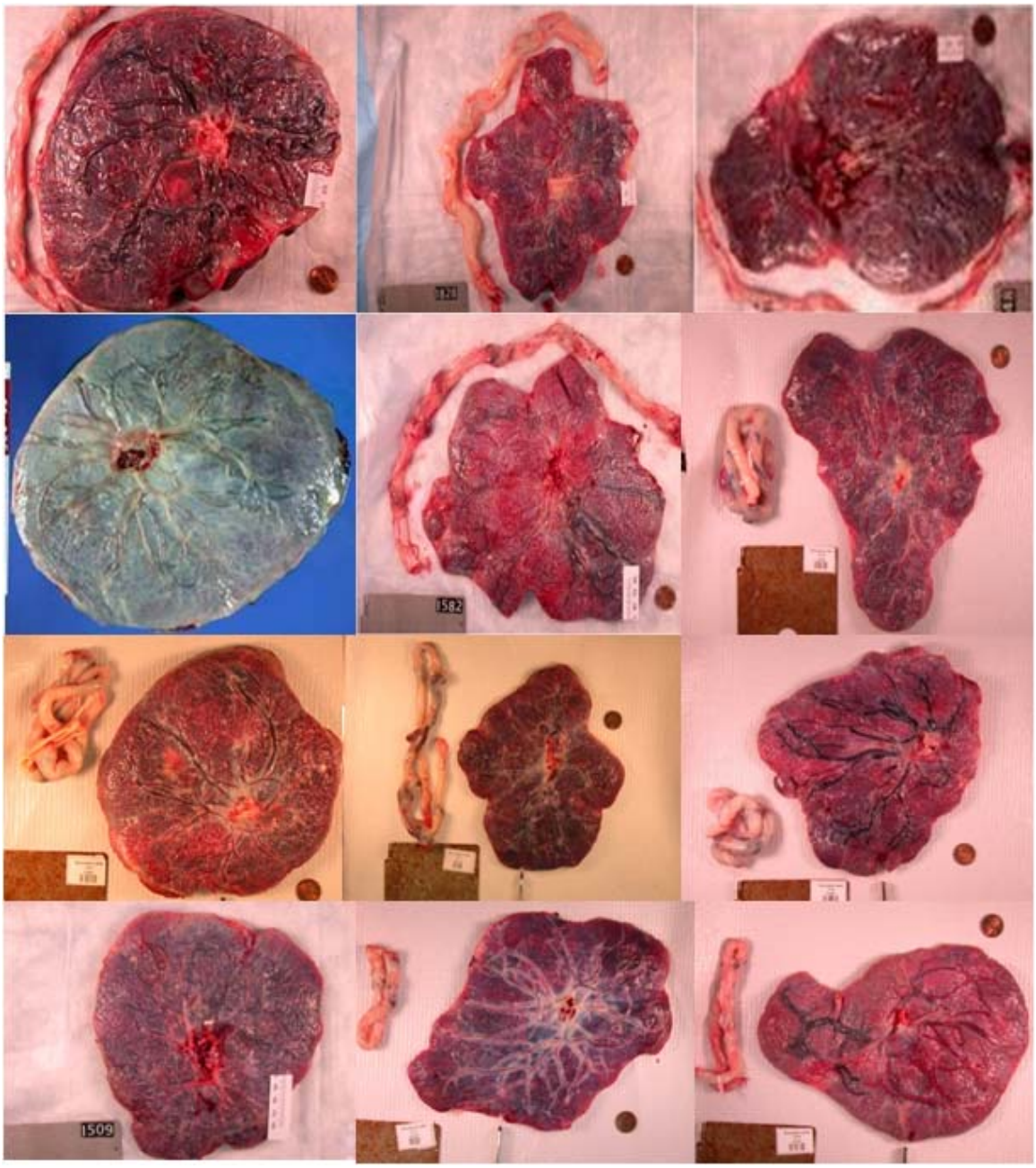


Examples of abnormal placental shapes that can be timed to gestational period prior to the mid trimester.

**Placental angiogenesis and ASD: Measureable difference in placental vascular structure.**

C Salafia MD MS, T Girardi PhD, C Newschaffer, PhD, R Miller, PhD, C Walker, MD, D Misra PhD, P Katzman, MD, J Moye, MD, M Fallin, PhD. I Herz-Picciotto, PhD, L Croen, PhD. Placental Modulation, Institute for Basic Research, Staten Island, NY, Placental Analytics LLC, Larchmont, NY, Drexel Autism Center, Philadelphia PA, Obs-Gyn, University of Rochester, Rochester NY, Obs/Gyn, UC Davis, Sacramento, CA, Family Medicine, Wayne State University, Detroit MI, Pathology, University of Rochester, Rochester NY, NCS, NICHD, Rockville, MD, Epidemiology, Bloomberg SPH, Baltimore MD, MIND Institute UC Davis, Sacramento CA, Kaiser Permanente, Oakland, CA.

**Hypothesis**. We hypothesize that vascular structure in placentas delivered in families with an older child diagnosed with autism (high risk) will differ from those of a series of unselected low-risk neonates.

**Materials and Methods**: 76 placentas from the National Children Study (NCS) and 33 from the Early Autism Risk Longitudinal Investigation (EARLI), had chorionic surface vasculature traced and analyzed for vascular network characteristics using nonparametric tests.

**Results**. EARLI vascular networks had significantly fewer branch generations, branch points and failed to extend toward the chorionic perimeter as did NCS networks, The distance between any artery and any vein was significantly greater in EARLI as compared to NCS (each $p<0.0001$). Representative arterivenous networks from an NCS (Figure 1) and an EARLI (Figure 2) placenta are shown below.

**Conclusions**: These data indicate a measurable difference in placental vascular network structure that can be quantified from a digital photograph in children at high risk for an eventual diagnosis of autism.

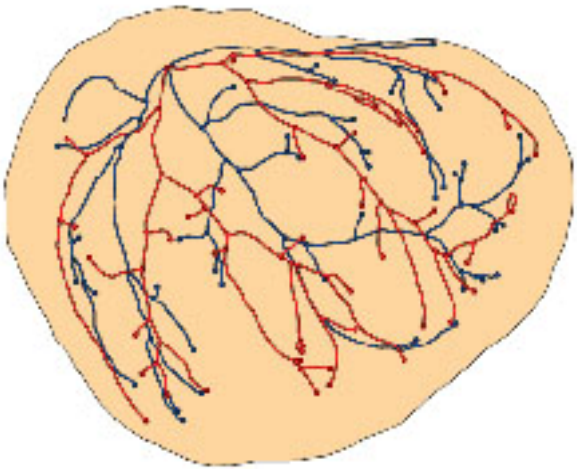

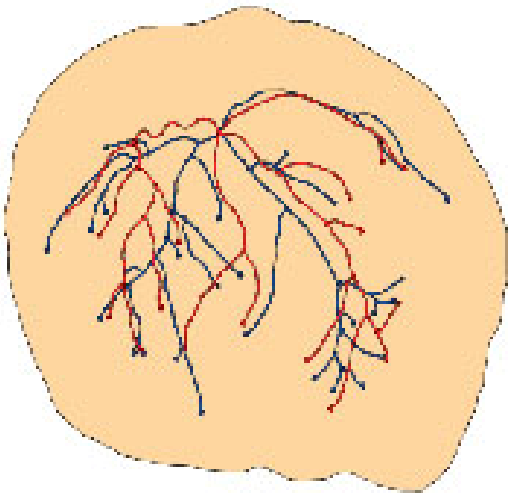

## CONCLUSIONS

The ALSPAC placenta sample remains the largest collection of placentas from a population cohort in which neurodevelopmental examinations were universally applied and placentas were archived. Despite the large number of deformed specimens, we have capitalized on our exhaustive analytic experience with the UNC-PIN study, the NCS Formative Research NIH-NCS-LOI-BIO-2-18 and the EARLI cohort to provided replicated evidence of aberrant early placental angiogenesis in terms of surface expansion and stem villous arborisation, and have new evidence of direct abnormality of chorionic vascular network, in terms of reduced branch generations and vascular surface density that may be vascular counterparts of the altered neuronal connectivity documented in ASD.

*Most importantly, our analyses confirm our hypothesis that placental structure varies between autism/ASD cases and in families with an autistic sibling, compared to a large birth cohort.*

**REFERENCES**


1. Salafia CM, Yampolsky M, Shlakhter A, Mandel DH, Schwartz N. Variety in placental shape: When does it originate? Placenta. 2012;33(3):164-170.
2. Yampolsky M, Salafia CM, Shlakhter O, Haas D, Eucker B, Thorp JM, MD. Modeling the variability of shapes of a human placenta. Placenta. 2008; 29(9):790-7.
3. Kleiber M. The Fire of Life. Revised ed. s.l. Robert E. Krieger Publ. Co.; 1975.
4. James GBW, Brown H, editors. Scaling in Biology. Santa Fe Institute studies in the sciences of complexity proceedings. New York, NY: Oxford University Press; 2000. p. 368.
5. Salafia CM, Maas E, Thorp JM, Eucker B, Pezzullo JC, Savitz DA. Measures of placental growth in relation to birth weight and gestational age. Am J Epidemiol. 2005 Nov 15; 162(10):991-8.
6. Yampolsky M, Salafia CM, Shlakhter O, Haas D, Eucker B, Thorp J. Centrality of the Umbilical Cord Insertion in a Human Placenta Influences the Placental Efficiency. Placenta. 2009 30(12): 1058-64.
7. Schwartz N, Mandel D, Shlakhter O, Coletta J, Pessel C, Timor-Tritsch IE, Salafia CM. Placental morphologic features and chorionic surface vasculature at term are highly correlated with 3-dimensional sonographic measurements at 11 to 14 weeks. J. Ultrasound Med. 2011 ;30(9):1171-8.
8. Yampolsky M, Salafia CM, Shlakhter O, Misra DP, Haas D, Eucker B, Thorp J. Variable placental thickness affects placental functional efficiency independent of other placental shape abnormalities. J Devel Origins Health Dis 2011;2(4):205-211.
9. Placental surface shape, function, and effects of maternal and fetal vascular pathology. Salafia CM, Yampolsky M, Misra DP, Shlakhter O, Haas D, Eucker B, Thorp J.Placenta. 2010 Nov; 31(11): 958-62.
10. Yampolsky M, Salafia CM, Shlakhter O, Haas D, Eucker B, Thorp J. Centrality of the Umbilical Cord Insertion in a Human Placenta Influences the Placental Efficiency. Placenta. 2009 30(12): 1058-64.
11. Misra DP, Salafia CM, Miller RK, Charles AK.Non-Linear and Gender-Specific Relationships Among Placental Growth Measures and The Fetoplacental Weight Ratio. Placenta. 2009 30(12): 1052-7.
12. Salafia CM, Misra DP, Yampolsky M, Charles AK, Miller RK. Allometric Metabolic Scaling and Fetal and Placental Weight. Placenta. 2009 Apr; 30(4): 355-60.
13. Salafia CM, Zhang J, Charles AK, Bresnahan M, Shrout P, Sun W, Maas EM. Placental characteristics and birthweight. Paed Perinat Epidemiol. 2008; 22(3): 229-39.
14. Baptiste-Roberts K, Salafia CM, Nicholson WK, Duggan A, Wang NY, Brancati FL. Gross placental measures and childhood growth. J Matern Fetal Neonatal Med. 2009;22(1):13-23.
15. Misra DP , Salafia CM, Charles AK, Miller RK.Birth weights smaller or larger than the placenta predict BMI and blood pressure at age 7 years. Journal of Developmental Origins of Health and Disease 2010;1(2):123-130.